

Short Communication

Influence of Wet Micro-Shot Peening on Surface Properties and Corrosion Resistance of AISI 304 Stainless Steel

Xinlong Wei^{1,*}, Dejia Zhu¹, Xiang Ling², Liang Yu¹, Min Dai¹.

¹ College of Mechanical Engineering, Yangzhou University, Yangzhou 225127, China

² School of Mechanical and Power Engineering, Nanjing Tech University, Nanjing 210009, China

*E-mail: xlwei@yzu.edu.cn

Received: 15 January 2018 / Accepted: 27 February 2018 / Published: 10 April 2018

As a new developed shot peening technology, wet micro shot peening is applied to investigate the influence on corrosion behavior of AISI 304 stainless steel in chloride solution using potentiodynamic polarization. Surface modifications including microstructure, residual stress, surface roughness and phase transformation are characterized. Results show that wet micro shot peening can promote the formation of deformation twins and deformation induced martensite, produce grain refinement, generate high magnitude compressive residual stress and increase surface roughness. Results of potentiodynamic polarization curves show that the specimen treated by lower peening pressure has better corrosion resistance than those of higher peening pressure treated and as-received specimen, but the higher peening pressure treated specimen affects inversely on the corrosion resistance with respect to as-received sample. Grain refinement and compressive residual stress induced by shot peening can enhance the corrosion resistance of AISI 304 stainless steel, but the surface roughness and deformation induced martensite generated during shot peening decrease the corrosion resistance. Corrosion resistance of AISI 304 stainless steel in chloride solution depends on the synergy effects of these factors.

Keywords: Wet micro shot peening; Microstructure; Surface roughness; Deformation induced martensite; Corrosion resistance

1. INTRODUCTION

Austenitic stainless steel is a very important category of materials for their outstanding mechanical properties and wide range of industrial applications. Despite the intrinsic high resistance of austenitic stainless steel to corrosion, it is critical to minimize corrosion for stable operation because austenitic stainless steel is extremely susceptible to local corrosion such as pitting and SCC in severe conditions of corrosive environment like chloride solution and tensile stresses [1-6].

Shot peening is an effective and common mechanical surface treatment to improve metallic components' fatigue properties and corrosion resistance by means of introducing severe plastic deformation and compressive residual stresses into the near surface region [7-10]. In addition to the traditional shot peening, recent technologies, such as laser shock peening [11-12], ultrasonic peening [13] and wet shot peening [14], have been developed and used widely. In particular, the laser shock peening treatment consists in irradiating surface of materials with nanosecond laser pulses that generate shock waves driven by plasma, which in turn lead to a certain amount of local plastic deformation [15]. Deep and high compressive residual stresses, limited roughening, and refined microstructure are usually the main characteristics of surfaces after laser shock peening treatment. Wei et al. [16] investigated the effects of laser shock peening on corrosion resistance of AISI 304 stainless steel in acid chloride solution and obtained the mechanism of corrosion resistance improvement by laser shock peening.

Generally, the variation of the roughness and grain refinement on the surface of metallic materials are induced by shot peening [17]. Surface roughness as a crucial surface feature plays a very important role in practical application. Several studies have been published indicating the significance of the roughness [18-20]. However, there is still insufficient information on corrosion properties after shot peening. Literatures on corrosion resistance after shot peening are conflicting without showing a clear trend [21-23]. Olumi et al. [21] reported that surface nanocrystallization induced by shot peening improved corrosion resistance. Nevertheless, Ahmed et al. [22, 23] found that shot peening induced higher surface roughness and reduced the corrosion resistance compared with the untreated materials.

As a new developed shot peening technology, wet micro shot peening is applied to investigate the effects on corrosion resistance of AISI 304 stainless steel in the present research. Surface modifications including microstructure, residual stress, surface roughness and martensite transformation are characterized. Furthermore, potentiodynamic polarization is used to evaluate the effects of wet micro shot peening on corrosion properties of AISI 304 stainless steel in chloride solution. The results are discussed and explained in detail.

2. EXPERIMENTAL

2.1 Specimens and wet micro shot peening experimental procedure

Table 1. Chemical composition of AISI 304 stainless steel

Element	C	Si	Mn	S	P	Cr	Ni	N	Fe
Content (wt.%)	0.046	0.51	1.06	0.004	0.025	18.32	8.04	0.05	Balance

Specimens were made from AISI 304 stainless steel plate with a thickness of 3 mm. The chemical composition of AISI 304 stainless steel was shown in Table 1. Prior to LSP treatment, specimens were grinded with silicon carbide (SiC) papers from 800 grit to 1500 grit, followed by cleaning in deionized water. Subsequently, the surfaces of specimens were degreased in ethanol by using ultrasonic cleaning.

Wet micro shot peening experiments were conducted using a mixture of ceramic balls with a diameter of 0.2 mm and water in the scale of 10 wt.%. Shots were propelled by air blast system into the path of high pressure air and accelerated through a blasting nozzle which was directed at the specimen. The peening pressures of 0.3-0.5 MPa were controlled by the setting pressure of air compressor. Moreover, the distance and angle between the nozzle and the surface of specimen were 100 mm and 90°, respectively. The peening coverage was 100%. After wet micro shot peening treatment, square corrosion specimens were cut from treated plate in dimensions of 10 mm × 10 mm × 3 mm, followed by being degreased in ethanol. Then, corrosion specimens were embedded in epoxy resin with a 1 cm² exposed area.

2.2 Surface modifications characterization

The Supra 55 field emission scanning electron microscope (SEM) was used to observe the microstructure of cross sections near the surface. The samples for surface microstructure observations were sectioned close to the treated area and carefully grinded to the mid-section and polished until there were no scratches on sample surface. After that, samples were etched using 10% mass fraction of oxalic acid solution in condition of 3 V voltage for 80 s at room temperature.

Surface residual stresses were performed by X-350A according to the $\sin^2\Psi$ method using Cr-K_α radiation. The diffraction plane was (220) crystallographic plane of the lattice of austenite [24, 25]. The X-ray beam diameter was about 1 mm. In the stress calculation, the Poisson's ratio was set to be 0.3. Diffracted intensities were acquired for tilting angles of 0°, 24.2°, 35.3° and 45° in four positions. The scanning starting angle and terminating angle were about 124° and 132°, respectively.

Surface roughness after wet micro shot peening expressed in arithmetic average R_a was measured by a Bruker Contour GT-K device.

The XRD qualitative analysis of martensite transformation of 304 stainless steel was performed by a Bruker X-ray diffraction equipment using Cu-K_α radiation. The generator was operated with 40 kV and 40 mA. The diffraction data were obtained over a 2θ range of 40-100° with a step by step scanning length of 0.02°. Using the 110, 200 reflections for martensite and 111, 200 reflections for austenite, the volume fraction V_α of α-martensite in the surface layer is evaluated using the following formula [26, 27]:

$$V_\alpha = \frac{\frac{1}{n} \sum_{j=1}^n \frac{I_\alpha^j}{R_\alpha^j}}{\frac{1}{n} \sum_{j=1}^n \frac{I_\gamma^j}{R_\gamma^j} + \frac{1}{n} \sum_{j=1}^n \frac{I_\alpha^j}{R_\alpha^j}} \quad (1)$$

where n , I and R are the number of peaks of the phase used in calculation, the integrated intensity of the reflecting plane and the material scattering factor, respectively.

2.3 Potentiodynamic polarization performance

Electrochemical potentiodynamic polarization experiments were performed by CHI660E, equipped with a standard three-electrode configuration: using a saturated calomel electrode (SCE) as the reference electrode and a platinum foil as the counter electrode. Electrochemical tests were performed in 3.5% NaCl at 30 °C. All the potentiodynamic polarization studies were conducted after stabilization of the open circuit potential (OCP). The scan rate used for polarization curves was fixed at 1 mV/s, which started from -250 mV (lower than OCP) to +800 mV (higher than OCP).

3. RESULTS AND DISCUSSION

3.1 Microstructure modifications

Fig. 1(a-d) shows the surface SEM morphologies of grains for samples after wet micro shot peening. The as-received specimen has a conventional γ -austenite microstructure. In the wet micro shot peened samples, deformation twins are clearly visible due to the relatively high plastic strain and the number of directions of deformation twins increases with increasing peening pressure of shot peening. Fig. 1(b) and 1(c) show that the intersection of deformation twins in two directions in original austenitic grains appears in the range of the distance in the depth of about 15 μm , which divide the original austenitic grains into a large number of submicron rhombic blocks. With the increase of the depth, the number of the deformation twins direction reduces and deformation twins in a single direction occur, which divide the original austenitic grains into parallel small platelets. Surface cumulative plastic strain increases with the peening pressure of shot peening, after 0.5 MPa shot peening treatment, the number of the twins direction grows and the intersection of deformation twins in three directions (as shown in Fig. 1(d)) appears at the surface, giving rise to submicron rhombic or triangular blocks.

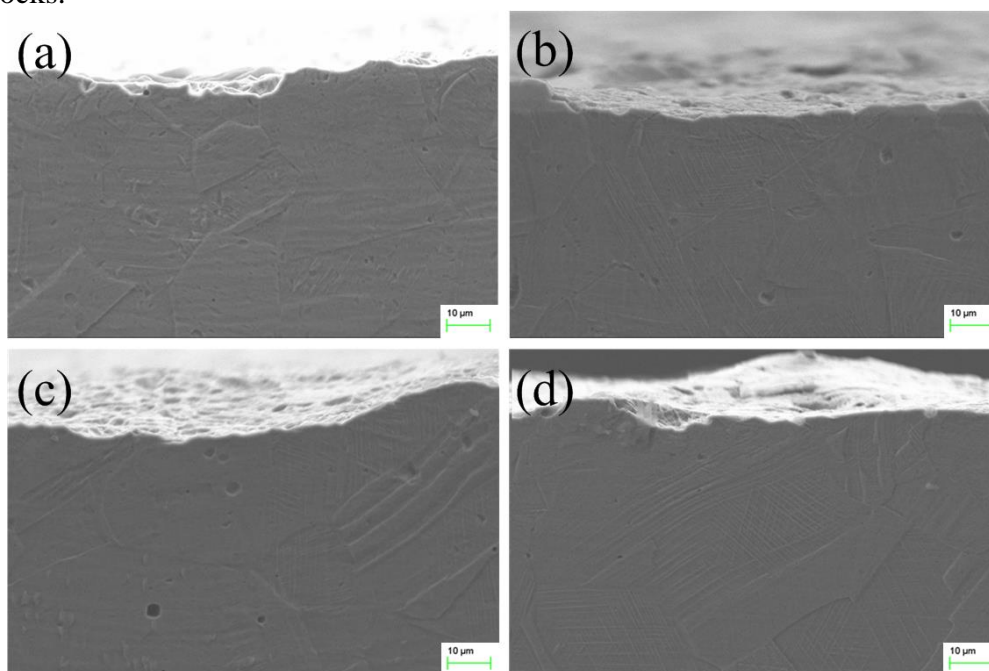


Figure 1. Cross sectional SEM morphologies of grains at various surface conditions with constant 100 mm nozzle specimen distance and 100% coverage: (a) as-received; (b) 0.3 MPa; (c) 0.4 MPa; (d) 0.5 MPa.

It can be concluded that after wet micro shot peening treatment, microstructure changes and varies with depth from the top surface and peening pressure of shot peening due to the intersection of deformation twins in different directions, generating submicron rhombic or triangular blocks, which implies the original grain refinement induced by wet micro shot peening.

3.2 Residual stress modifications

Residual stresses are usually known to be the key to enhanced mechanical properties such as fatigue, corrosion and stress corrosion cracking resistance. Table 2 shows the measured surface residual stresses after wet micro shot peening. Prior to shot peening treatment, the as-received specimen shows residual stress at the surface amounting to about -27 MPa, which is produced most probably due to the specimen preparation. According to Table 2, surface residual stress after shot peening varies from -313.7 MPa to -392.1 MPa with increasing the peening pressure from 0.3 MPa to 0.5 MPa. Obviously, it can be seen that the surface residual stress could be significantly modified from smaller compressive stress for as-received sample to high magnitude compressive stress after shot peening treatment, which can improve electrochemical corrosion resistance of 304 stainless [16].

Table 2. Surface residual stresses of samples for different shot peening treatment

Specimen	As-received	0.3 MPa	0.4 MPa	0.5 MPa
Residual stresses / MPa	-27	-313.7	-345.9	-392.1

3.3 Surface roughness

The 3D contour plots of surface roughness before and after shot peening are shown in Fig. 2. It can be seen from Fig. 2(a) that the surface before wet micro shot peening is smooth and the polishing scratches are arranged in a straight line. However, the polishing scratches disappear and the rough surface is induced by shot peening due to the severe bombardment by ceramic balls, as shown in Fig. 2(b)-2(d). The surface roughness values are listed in Table 3. The fact that surface roughness increases after shot peening is verified by roughness variation from 0.304 μm R_a for grinded surface to 2.930 μm R_a after shot peening with 0.3 MPa peening pressure. As clear from Table 3, the surface roughness increases gradually from 2.930 μm R_a to 3.110 μm R_a with increasing the peening pressure from 0.3 MPa to 0.5 MPa, which may be attributed the increased kinetic energy of ceramic balls for higher peening pressure that lead to a more severely deformed surface.

Table 3. Surface roughness values at different surface conditions

Specimen	As-received	0.3 MPa	0.4 MPa	0.5 MPa
$R_a / \mu\text{m}$	0.304	2.930	3.016	3.110

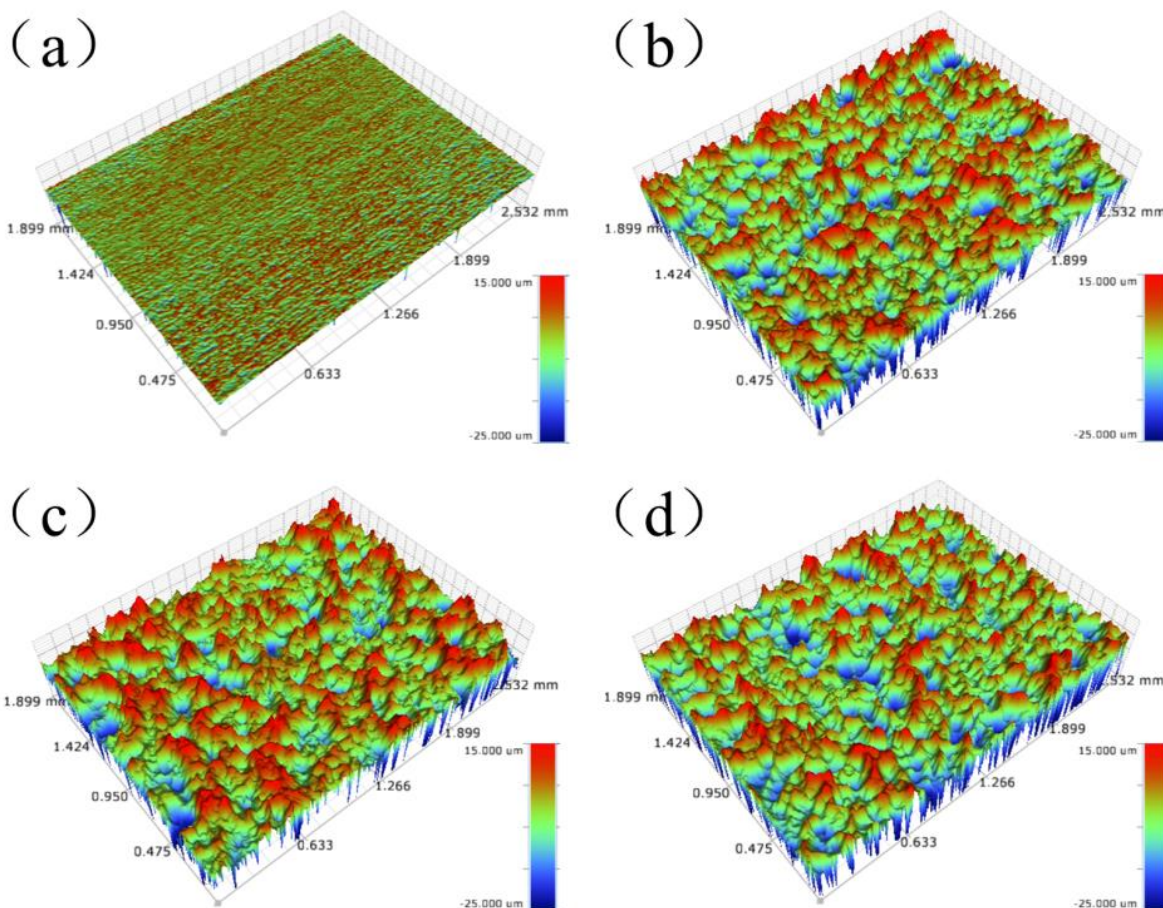


Figure 2. Surface roughness of specimens at various surface conditions with constant 100 mm nozzle specimen distance and 100% coverage: (a) as-received; (b) 0.3 MPa; (c) 0.4 MPa; (d) 0.5 MPa.

3.4 XRD

Fig.3 shows the surface XRD patterns of AISI 304 stainless steel treated by different peening pressures of wet micro shot peening. Sample without treatment only consists of the austenite phase, while the transformation of austenite to α -martensite has occurred during shot peening treatment. Unlike untreated 304 stainless steel, sample treated by shot peening consists of a mixture of both austenite and martensite phase, which clearly shows that only wet micro shot peening treatment generates the martensite phase. The volume fraction of α -martensite of the treated samples shows a strong dependence on the extent of deformation, which is a function of peening pressures. The volume fraction of α -martensite increases with increasing peening pressure. According to Eq. (1), the volume fraction V_{α} can be determined to be about 26.74% for 0.3 MPa, 31.12% for 0.4 MPa and 34.48% for 0.5 MPa, respectively.

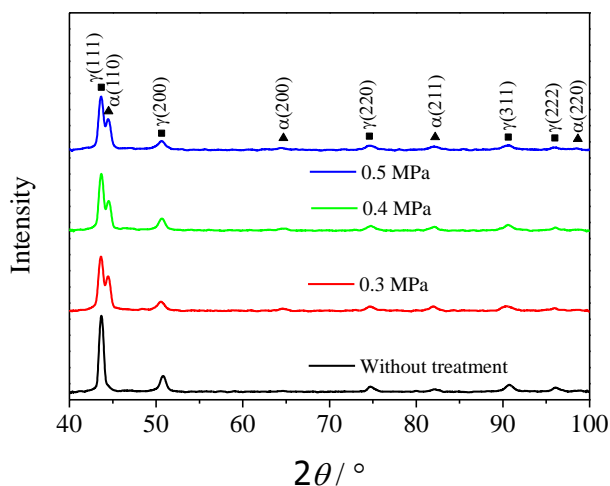


Figure 3. XRD patterns for different surface conditions with constant 100 mm nozzle specimen distance and 100% coverage.

3.5 Corrosion behavior

The corrosion current density (i_{cor}), corrosion potential (E_{cor}) and cathodic Tafel slopes (B_c) of each sample is determined from potentiodynamic polarization curves, and the results are shown in Table 4. After wet micro shot peening with 0.3 MPa peening pressure, the corrosion current density decreases to $0.420 \mu\text{A cm}^{-2}$ compared with $1.137 \mu\text{A cm}^{-2}$ for as-received specimen, and the corrosion potential is shifted slightly towards positive direction. However, after shot peening with increasing peening pressure, the corrosion current densities increase to $1.236 \mu\text{A cm}^{-2}$ for 0.4 MPa and $1.313 \mu\text{A cm}^{-2}$ for 0.5 MPa, respectively.

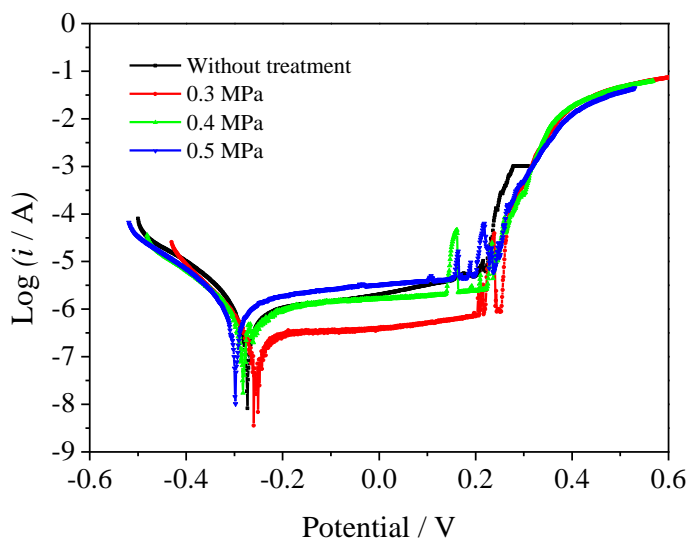


Figure 4. Potentiodynamic polarization curves for different peening pressures with constant 100 mm nozzle specimen distance and 100% coverage.

Also, the corrosion potential is shifted slightly towards negative direction when increasing peening pressure. The smaller values of the corrosion current density imply higher corrosion resistance.

In addition, the more positive values of the corrosion potential are, the better corrosion resistance is. Hence, the specimen treated by lower peening pressure has better corrosion resistance than those of higher peening pressure treated and non-treated specimen, but the higher peening pressure treated specimen affects inversely on the corrosion resistance with respect to as-received sample.

Table 4. Results of polarization curves at different peening pressures

Specimen	Current density / $\mu\text{A cm}^{-2}$	Corrosion potential / V	Cathodic Tafel slopes / V dec^{-1}
As-received	1.137	-0.273	-8.330
0.3 MPa	0.420	-0.260	-9.928
0.4 MPa	1.236	-0.282	-8.054
0.5 MPa	1.313	-0.298	-8.163

Surface characteristics such as grain refinement, compressive residual stress, surface roughness and deformation induced martensite induced by wet micro shot peening have been attributed to account for modifications of corrosion resistance of AISI 304 stainless steel. In case of the stainless steels, grain refinement means the increase in density of grain boundaries, which can promote Cr diffusion to the surface of the material and generate the formation of homogenous and dense passive film rich in Cr that may obtain a better corrosion resistance [28]. The presence of compressive residual stress can also increase corrosion resistance. Liu and Frankel [29] have founded that compressive residual stress would decrease the passive current density of AA2024-T3 Al alloy in 1 M NaCl. The detrimental influence of surface roughness and deformation induced martensite on the corrosion resistance of stainless steel has also been found [22,23,30,31]. Mordyuk et al. [31] have reported that the deformation induced martensite produce a galvanic effect between austenite and martensite phases. It is clear that grain refinement and compressive residual stress induced by wet micro shot peening can enhance the corrosion resistance of AISI 304 stainless steel. The surface roughness and deformation induced martensite generated during shot peening treatment would decrease the corrosion resistance. Corrosion resistance of the 304 stainless steel in chloride solution depends on the synergy effects of these factors. For samples after lower peening pressure treatment of 0.3 MPa, grain refinement and compressive residual stress induced by shot peening have advantages over detrimental influence caused by surface roughness and deformation induced martensite. However, for samples increasing peening pressure, a rougher surface and higher volume fraction of deformation induced martensite would strengthen the detrimental influence and nullify the beneficial effects of grain refinement and compressive residual stress on corrosion resistance.

4. CONCLUSIONS

The effects of wet micro shot peening on corrosion behavior of AISI 304 stainless steel in chloride solution have been investigated using potentiodynamic polarization experiments. Surface modifications including microstructure, residual stress, surface roughness and phase transformation are characterized. The results obtained are itemized as follows:

(1) Surface microstructure after wet micro shot peening treatment presents deformation twins and varies with depth from the top surface and peening pressure due to the intersection of deformation twins in different directions, which lead to original austenitic grain refinement near the surface.

(2) Wet micro shot peening can introduce high magnitude compressive residual stress at the surface of the 304 stainless steel. Surface residual stress after shot peening varies from -313.7 MPa to -392.1 MPa with increasing peening pressure from 0.3 MPa to 0.5 MPa.

(3) Wet micro shot peening increases surface roughness and enables phase transformation from austenite to martensite. Surface roughness increases from 0.304 μm R_a for grinded surface to about 3 μm R_a after shot peening. The volume fraction V_α can be determined to be about 26.74% for 0.3 MPa, 31.12% for 0.4 MPa and 34.48% for 0.5 MPa, respectively.

(4) The effects of wet micro shot peening on corrosion resistance are conflicting. Results of potentiodynamic polarization curves show that the specimen treated by lower peening pressure has better corrosion resistance than those of higher peening pressure treated and non-treated specimen, but the higher peening pressure treated specimen affects inversely on the corrosion resistance with respect to as-received sample.

(5) Grain refinement and compressive residual stress induced by wet micro shot peening can enhance the corrosion resistance of AISI 304 stainless steel, but the surface roughness and deformation induced martensite generated during shot peening treatment would decrease the corrosion resistance. Corrosion resistance of the 304 stainless steel in chloride solution depends on the synergy effects of these factors.

ACKNOWLEDGEMENTS

The financial supports of the Science and Technology Innovation Cultivation Fund Project of Yangzhou University (No. 2017CXJ023 and No. 2016CXJ020) and the Research Innovation Program of Graduated Student of Jiangsu Province (No. KYZZ_0221) are gratefully acknowledged by the authors. The Jiangsu Province Basic Research Program under Grant (No. BK20160474) and Natural Science Fund for Colleges and Universities in Jiangsu Province under Grant (No. 16KJB460024) are also acknowledged.

References

1. R. Nishimura, A. Sulaiman, Y. Maeda, *Corros. Sci.*, 45 (2003) 465.
2. O. M. Alyousif, R. Nishimura, *Corros. Sci.*, 49 (2007) 3040.
3. O. M. Alyousif, R. Nishimura, *Corros. Sci.*, 50 (2008) 2919.
4. H. S. Costa-Mattos, I. N. Bastos, J. A. C. P. Gomes, *Corros. Sci.*, 50 (2008) 2858.
5. P. D. Tiedra, O. Martin, *Mater. Design*, 49 (2013) 103.
6. A. A. Aghuy, M. Zakeri, M. H. Moayed, M. Mazinani, *Corros. Sci.* 94 (2015) 368.
7. D. J. Chadwick, S. Ghanbari, D. F. Bahr, M. D. Sangid, *Fatigue Fract. Eng. M.*, 41 (2018) 71.
8. K. Takahashi, K. Iwanaka, H. Koike, *Mater. Sci. Tech.-Lond.*, 33 (2017) 623.
9. J. Gan, D. Sun, Z. Wang, P. Luo, W. G. Wu, *J. Constr. Steel Res.*, 126 (2016) 74.
10. T. S. Wang, J. K. Yu, B. F. Dong, *Surf. Coat. Tech.*, 200 (2006) 4777.
11. Y. Sano, M. Obata, T. Kubo, N. Mukai, M. Yoda, K. Masaki, Y. Ochi, *Mat. Sci. Eng. A-Struct.*, 417 (2006) 334.
12. X. L. Wei, X. Ling, *Appl. Surf. Sci.*, 301 (2014) 557.

13. S. Kumar, K. Chattopadhyay, V. Singh, *J. Alloy. Compd.*, 724 (2017) 187.
14. K. Li, X. S. Fu, R. D. Li, P. T. Gai, Z. Q. Li, W. L. Zhou, G. Q. Chen, *Int. J. Fatigue*, 85 (2016) 65.
15. X. L. Wei, J. X. Zhou, X. Ling, *Laser. Eng.*, 27 (2014) 347.
16. X. L. Wei, C. Zhang, X. Ling, *J. Alloy. Compd.*, 723 (2017) 237.
17. H. S. Lee, D. S. Kim, J. S. Jung, Y. S. Pyoun, K. Shin, *Corros. Sci.*, 51 (2009) 2826.
18. H. Wieser, *Mater. Corros.*, 55 (2004) 186.
19. M. Mhaede, *Mater. Design*, 41 (2012) 61.
20. M. Abdulstaar, M. Mhaede, M. Wollmann, L. Wagner, *Surf. Coat. Tech.*, 254 (2014) 244.
21. S. Olumi, S. K. Sadrnezhad, M. Atai, *J. Mater. Eng. Perform.*, 24 (2015) 3093.
22. A. A. Ahmed, M. Mhaede, M. Wollmann, L. Wagner, *Appl. Surf. Sci.*, 363 (2016) 50.
23. A. A. Ahmed, M. Mhaede, M. Basha, M. Wollmann, L. Wagner, *Surf. Coat. Tech.*, 280 (2015) 347.
24. J. Johansson, M. Oden, X. H. Zeng, *Acta Mater.*, 47 (1999) 2669.
25. A. Zambon, P. Ferro, F. Bonollo, *Mat. Sci. Eng. A*, 424 (2006) 117.
26. A. K. De, D. C. Murdock, M. C. Mataya, J. G. Speer, D. K. Matlock, *Scripta Mater.*, 50 (2004) 1445.
27. B. N. Mordyuk, G. I. Prokopenko, M. A. Vasylyev, M. O. Lefimov, *Mat. Sci. Eng. A*, 458 (2007) 253.
28. W. Ye, Y. Li, F. H. Wang, *Electrochim. Acta*, 54 (2009) 1339.
29. X. D. Liu, G. S. Frankel, *Corros. Sci.* 48 (2006) 3309.
30. A. Barbucci, M. Delucchi, M. Panizza, M. Sacco, G. Cerisola, *J. Alloy. Compd.*, 317–318 (2001) 607.
31. B. N. Mordyuk, G. I. Prokopenko, M. A. Vasylyev, M. O. Lefimov, *Mat. Sci. Eng. A*, 458 (2007) 253.

© 2018 The Authors. Published by ESG (www.electrochemsci.org). This article is an open access article distributed under the terms and conditions of the Creative Commons Attribution license (<http://creativecommons.org/licenses/by/4.0/>).